

Antiparticle sources for antihydrogen production and trapping

M Charlton¹, G B Andresen², M D Ashkezari³, M Baquero-Ruiz⁴, W Bertsche¹, P D Bowe², C C Bray⁴, E Butler¹, C L Cesar⁵, S Chapman⁴, J Fajans⁴, T Friesen⁶, M C Fujiwara⁷, D R Gill⁷, J S Hangst², W N Hardy⁸, R S Hayano⁹, M E Hayden³, A J Humphries¹, R Hydomako⁶, S Jonsell^{1,10}, L V Jørgensen¹, S J Kerrigan¹, L Kurchaninov⁷, R Lambo⁵, N Madsen¹, S Menary¹¹, P Nolan¹², K Olchanski⁷, A Povilus⁴, P Pusa¹², F Robicheaux¹³, E Sarid¹⁴, S Seif El Nasr⁸, D M Silveira^{9,15}, C So⁴, J W Storey⁷, R I Thompson⁶, D P van der Werf¹, D Wilding¹, J S Wurtele⁴ and Y Yamazaki¹⁵ (ALPHA Collaboration)

¹ Department of Physics, Swansea University, Swansea SA2 8PP, United Kingdom

² Department of Physics and Astronomy, Aarhus University, DK-8000 Aarhus C, Denmark

³ Department of Physics, Simon Fraser University, Burnaby BC, V5A 1S6, Canada

⁴ Department of Physics, University of California, Berkeley, CA 94720-7300, USA

⁵ Instituto de Física, Universidade Federal do Rio de Janeiro, Rio de Janeiro 21941-972, Brazil

⁶ Department of Physics and Astronomy, University of Calgary, Calgary AB, T2N 1N4, Canada

⁷ TRIUMF, 4004 Wesbrook Mall, Vancouver BC, V6T 2A3, Canada

⁸ Department of Physics and Astronomy, University of British Columbia, Vancouver BC, V6T 1Z4, Canada

⁹ Department of Physics, University of Tokyo, Tokyo 113-0033, Japan

¹⁰ Fysikum, Stockholm University, SE-10609, Stockholm, Sweden

¹¹ Department of Physics and Astronomy, York University, Toronto, ON, M3J 1P3, Canada

¹² Department of Physics, University of Liverpool, Liverpool L69 7ZE, United Kingdom

¹³ Department of Physics, Auburn University, Auburn, AL 36849-5311, USA

¹⁴ Department of Physics, NRCN-Nuclear Research Center Negev, Beer Sheva, IL-84190, Israel

¹⁵ Atomic Physics Laboratory, RIKEN, Saitama 351-0198, Japan

E-mail: M.Charlton@Swansea.ac.uk

Abstract. Sources of positrons and antiprotons that are currently used for the formation of antihydrogen with low kinetic energies are reviewed, mostly in the context of the ALPHA collaboration and its predecessor ATHENA. The experiments were undertaken at the Antiproton Decelerator facility, which is located at CERN. Operations performed on the clouds of antiparticles to facilitate their mixing to produce antihydrogen are described. These include accumulation, cooling and manipulation. The formation of antihydrogen and some of the characteristics of the anti-atoms that are created are discussed. Prospects for trapping antihydrogen in a magnetic minimum trap, as envisaged by the ALPHA collaboration, are reviewed.

1. Introduction

The controlled formation of antihydrogen by the interaction of cold clouds of antiprotons and positrons has become routine since 2002, when the first successful experiments were reported by the ATHENA [1] and ATRAP [2] collaborations. Several investigations have been performed since which have shed light on the antihydrogen created under the conditions of these two experiments, which typically involved mixing antiprotons with positron plasmas in Penning traps, with their concomitant electric and strong magnetic fields. The work has included experiment, theory and simulation. The individual references to these studies are too numerous to list here; the interested reader is referred to the following articles, where much of the work is synthesised or reviewed [3, 4, 5, 6].

The motivation for producing antihydrogen is to eventually compare its properties with those of hydrogen. In spectroscopic terms, the 1S-2S two-photon [7], and the ground state hyperfine [8] transitions in atomic hydrogen are some of the best known quantities in physics, and it is these lines which are a natural starting point for antihydrogen spectroscopy. Furthermore, experimental studies of the gravitational interaction of antimatter with matter have never been performed, and will surely be a focus of experimental attention [9, 10]. Theoretical motivation for the latter has been summarised elsewhere [3], whilst extensions to the Standard Model of Particle Physics to incorporate effects which may produce spectral shifts between the lines of hydrogen and antihydrogen (i.e. CPT violation) have been given by Kostelecký and co-workers and others [11, 12, 13, 14].

In several of the experimental approaches to comparisons of hydrogen and antihydrogen (and in particular spectroscopy), it is envisaged that the latter needs to be held in a neutral atom trap to prolong its interaction with the interrogating fields. This is the approach being taken by the ALPHA and ATRAP collaborations that are both actively pursuing antihydrogen trapping using modified versions of the classic Ioffe-Pritchard magnetic minimum trap [15], superimposed upon the apparatus they use to produce the anti-atoms [16, 17]. Here we will describe the ALPHA apparatus and approach.

The remainder of this contribution is comprised of summaries of the techniques used by ALPHA to confine and manipulate positron and antiproton clouds and the production of antihydrogen atoms in their current neutral atom trapping apparatus. Progress towards the trapping of antihydrogen will be briefly discussed.

2. Antiproton capture and manipulation

The antiprotons used in the antihydrogen studies emanate from the Antiproton Decelerator (AD) facility [18], which is located at the European Particle Physics Laboratory, CERN. This facility is unique worldwide as it decelerates stored antiprotons to a kinetic energy of around 5.3 MeV and supplies them to the experiments in pulses around 100 ns wide, each containing just over 10^7 particles, every 100 seconds or so. A simple, but well established, foil-moderation technique [19] is used to reduce the kinetic energy of the antiprotons on entry to the ALPHA apparatus. A fraction of the antiprotons ($\sim 10^{-2}$ - 10^{-3}) emerge from the foil with kinetic energies which allow them to be dynamically captured in a Penning-type trap (the so-called catching trap) in which radial confinement is provided by a strong axial magnetic field (typically around 3 T), whilst axial confinement is achieved by electric fields which are suitably pulsed to allow the antiprotons to enter, but not escape. In this manner around 40,000 antiprotons can be captured per AD shot. A schematic illustration of the ALPHA apparatus is given in figure 1, with the strength of the axial component of the magnetic field shown in the lower box.

Before the antiproton pulse arrives a cloud of electrons with a density of 10^8 - 10^9 cm^{-3} is loaded into the catching trap. These cool rapidly [20] via the emission of synchrotron radiation in the strong magnetic field and, in the absence of any sources of heat, will reach equilibrium with the temperature of the surrounding trap electrodes, which in the case of ALPHA is ~ 7

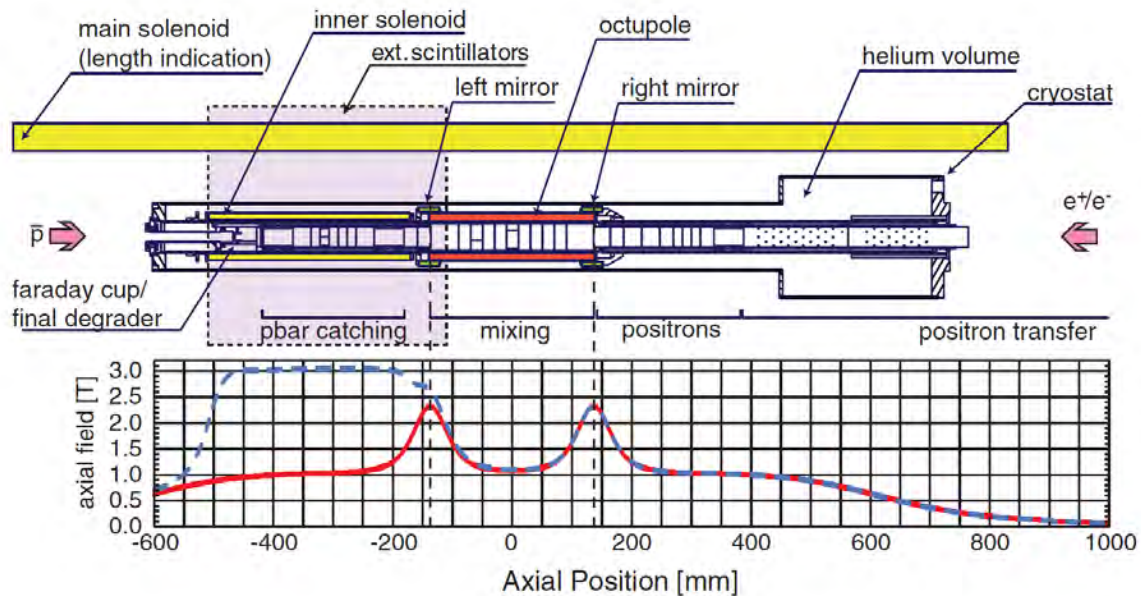


Figure 1. Schematic illustration of the antiproton capture and antihydrogen formation sections of the ALPHA apparatus, with a section through the magnetic coil system. The positron accumulator is located to the right of this apparatus. The positions of external scintillators used to monitor antiproton and antihydrogen annihilations are shown, though the inner antiproton annihilation vertex detector is omitted for clarity. The lower panel shows the behaviour of B_z , the axial magnetic field. The radial component (not shown) is provided by the octupole.

K. (We note here that it is very challenging to achieve such low electron plasma temperatures. For instance, since plasma expansion due to trap imperfections [21, 22] is difficult to eliminate, Joule heating will raise the temperature of the cloud.) The trapped antiprotons, confined to the axis of the instrument, lose kinetic energy to the colder electron cloud, and within a few seconds reach equilibrium and reside in the same potential well as the electrons [23]. The electrons can be removed, if desired, by rapidly lowering the confining potential, though this manipulation may also result in a somewhat heated antiproton ensemble. In ALPHA, the antiprotons are initially captured in the 3 T region to the left of figure 1 to enhance the efficiency [24], before being transferred to the 1 T region for mixing to form antihydrogen. As well as further electron cooling, other manipulations are performed on the antiprotons once they reside in this region, as will be described.

One of the major problems facing the antihydrogen field is to trap the anti-atoms for further study. As will be described in section 4, the neutral atom traps used in this effort, based upon the magnetic minimum principle [15], are only ~ 1 K deep. Thus, the antihydrogen must be created at a temperature which will allow as much as possible to be captured into these shallow traps. The antihydrogen is typically formed via positron-antiproton interactions in a positron plasma which may have a density around 10^8 cm^{-3} . The plasma will have a self radial electric field, E_r , given by $E_r = n_e e r / 2\epsilon_0$, where n_e is the plasma density, r is the radius in the plasma (up to the edge at r_p) and e and ϵ_0 have their usual meanings. When this electric field is combined with the axial magnetic field, B_z , a tangential drift speed results, given by E_r/B_z , as the plasma rotates about the axis with a constant angular frequency. It is easily seen that, to leading order (e.g. [6]), the rotation speed is independent of mass such that the antiprotons will co-rotate with the positrons. Such motion will add extra kinetic energy to the antiproton which

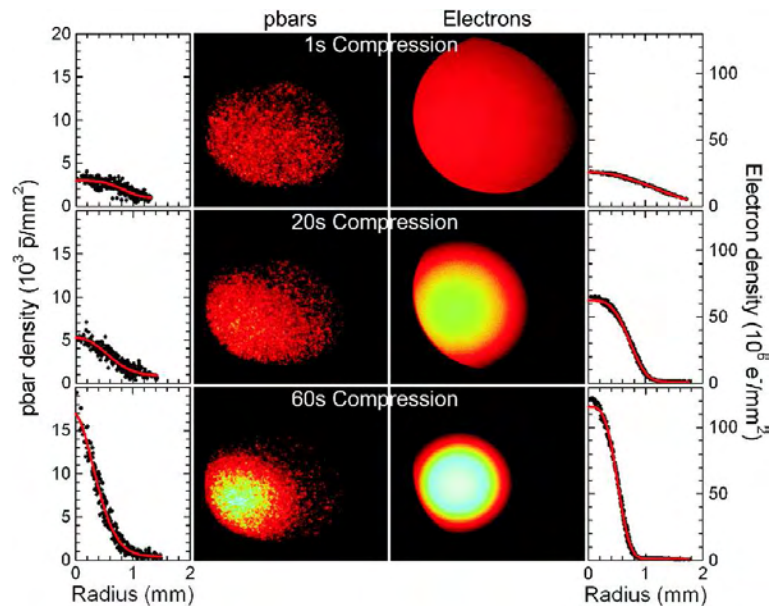


Figure 2. Examples of images of the antiproton and electron clouds for three different compression times, including the respective radial profiles. The images were obtained using an MCP/phosphor screen arrangement similar to that shown in figure 4a. The electrons were initially captured into a 136 mm long trap. Typical antiproton samples contained $\sim 3 \times 10^4$ particles.

will transfer to the antihydrogen and be dependent upon the radial position of production of the anti-atom in the plasma. For typical examples of $n_e = 10^8 \text{ cm}^{-3}$, $r = 1 \text{ mm}$ and $B_z = 1 \text{ T}$, it can be found that the extra kinetic energy is several 10s of degrees K, and thus much larger than the typical trap depths.

Thus, ALPHA has developed a technique to control the radial extent of the antiprotons using a variant of the rotating wall technique which has been used successfully over a decade or more to manipulate the radial profile of a number of plasma species, including positrons: see e.g. [25, 26, 27, 28, 29, 30, 31]. The technique involves using controlled compression of an electron plasma in which the antiprotons are embedded [32]. The rotating wall was achieved using a fixed frequency of typically 10 MHz applied to an azimuthally segmented electrode located in the 3T region of the ALPHA apparatus. The radial profiles of the antiprotons and electrons could be measured by individually ejecting each cloud onto a multi-channel plate/phosphor imaging system located upstream in a low magnetic field region.

Examples of the compression are presented in figure 2, which shows the progressive narrowing of the radial profile of the electron and antiproton clouds; see [32] for more details. Figure 3 shows the tracking of the radii of the respective clouds with compression time. Note that if the electron compression is undertaken too rapidly, the antiprotons do not track their behaviour. In this instance, it is likely that they quickly find themselves in a region of very low electron density, such that they can no longer couple via collisions. Reductions in areal density of a factor of 10 have been achieved, which translates directly into an order of magnitude decrease in the temperature due to rotational effects, with an accompanying reduction in the antihydrogen temperature. Compressed antiproton clouds are also beneficial in that they ensure complete spatial overlap with the positron plasma and help maintain the stability of the cloud against radial drift in the presence of the magnetic minimum field (see section 4).

It is also notable that manoeuvring the antiprotons from trap-to-trap (obviously using

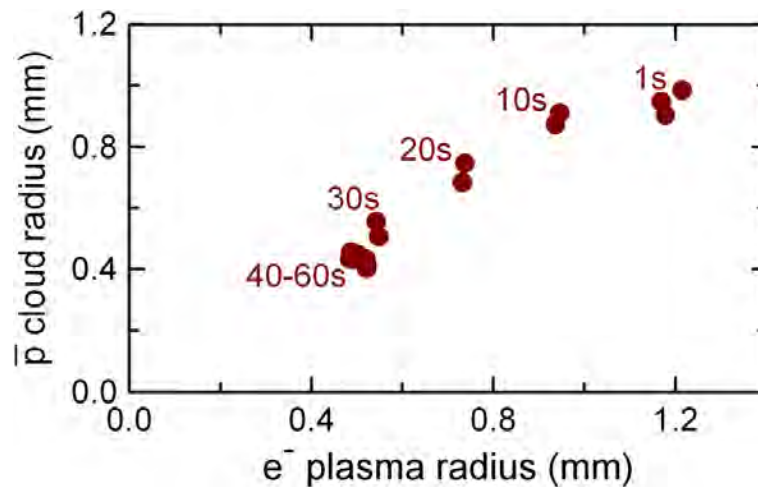


Figure 3. The tracking of the radii of the electron plasma and the antiproton cloud during sympathetic compression for various durations as indicated.

electric fields to accelerate and then decelerate and re-trap them) can lead to increases in the temperature of a cold ensemble. Re-cooling with electrons is always feasible, but ejecting these before antihydrogen experiments can take place can, as mentioned above, also heat the antiprotons. ALPHA has recently [33] developed a technique familiar in cold atom physics, namely evaporative cooling, to reduce the antiproton temperature into the cryogenic regime, and has directly measured such low antiproton temperatures for the first time.

The part of the ALPHA apparatus used for this work, and examples of some of the potential wells used, are illustrated schematically in figure 4. The potential well holding the antiprotons could be progressively lowered, and, allowing time after each step for the remaining cloud to re-thermalise via collisions, the temperature of the remaining ensemble was reduced. The temperature could be measured by slowly allowing the antiprotons to escape from the cloud, to be detected by the downstream MCP/phosphor arrangement. The first antiprotons to escape will be from the exponential tail of the Maxwell-Boltzmann distribution, such that the slope of a logarithmic plot of the integrated counts can be used to derive the temperature of the trapped cloud. Such a technique has been in use in non-neutral plasma physics for some time [34], and examples plots are shown in figure 5. It can be seen that lowering the antiproton well carefully to 10 mV produces a (9 ± 4) K ensemble, with the uncertainty mainly due to that on the voltages applied to the traps. It is notable that at this low trap depth/temperature, (6 ± 1) % of the antiprotons remained trapped.

3. Positron capture and manipulation

The positron accumulator, and most of the associated methodology, used by the ALPHA collaboration was developed for the predecessor ATHENA experiment. Much of this has been described briefly elsewhere [30, 35], though there is no major journal account of the device and its performance.

The ALPHA positron apparatus is shown schematically in figure 6. The beamline is based around a ^{22}Na β^+ source and a conical [36] solid neon moderator [37], which is attached to, though electrically isolated from, a closed cycle helium refrigerator. The latter could reach temperatures around 5 K, and with the neon optimally plated onto the source/cone arrangement, low energy (\sim few eV) positrons were emitted with a yield of around $2 \times 10^5 e^+ s^{-1} \text{mCi}^{-1}$. The low energy positrons were guided at a kinetic energy of around 80 eV using magnetic fields to

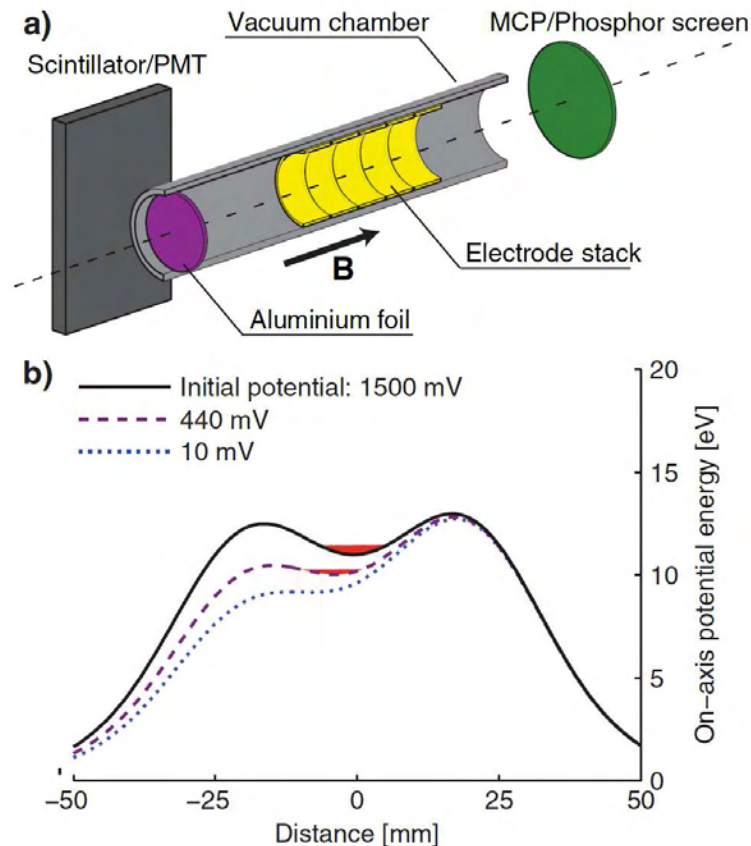


Figure 4. (a) Schematic of the part of the ALPHA apparatus used to investigate the evaporative cooling of antiprotons. (b) Three examples of the confining potential wells used in the experiments. The shallowest well (10 mV) was that which achieved the lowest antiproton temperature of ~ 9 K (see text).

the 3-stage buffer gas Penning-Malmberg trap of the type pioneered by Surko and co-workers [38, 39, 40].

Collisions with the nitrogen buffer gas cause a fraction, ϵ , of the positrons to lose kinetic energy whilst traversing the 3-stage electrode arrangement and become trapped. As a result of further collisions with the nitrogen gas in the second and third stages of the trap, the positrons eventually reside in the latter, where they accumulate. The addition of a cooling gas to the third stage, typically CF_4 , SF_6 , or CO_2 , with a high thermalisation rate for positrons (see e.g. [41, 42]) is useful as it allows more effective rotating wall compression of the cloud. However, a cooling gas is typically not applied during antihydrogen production runs, as the pumpout time (see below) becomes extended. The accumulator rotating wall is typically applied for the full 200 s of the accumulation time at a frequency of around 600 kHz. Once accumulation is complete, the nitrogen buffer gas is pumped out [43], and after about 20-30 s the pressure is low enough for the positrons to be ballistically transported [30] to the main system (figure 1) and recaptured. The positrons cool in the strong axial magnetic field of the mixing region solenoid via the emission of synchrotron radiation and are compressed using a second rotating wall system which operates at a frequency of 700 kHz for a period of around 100 s.

In controlling the positrons, and their eventual interaction with the antiprotons, it has been found useful to reduce their overall number. This reduces the positron density, such that the

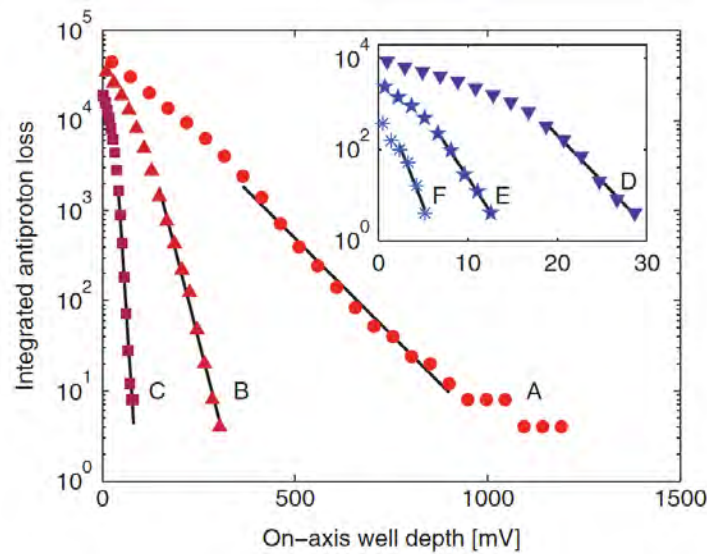


Figure 5. Integrated antiproton loss as the respective potential wells are lowered. The lines are the exponential fits used to deduce the antiproton temperature in each case. The data correspond, from A to F, to antiproton temperatures of 1040, 325, 57, 23, 19 and 9 K, respectively. Before each cooling experiment a cloud of $\sim 45,000$ antiprotons with a radius of 0.6 mm and a density of $7.5 \times 10^6 \text{ cm}^{-3}$ was prepared [33].

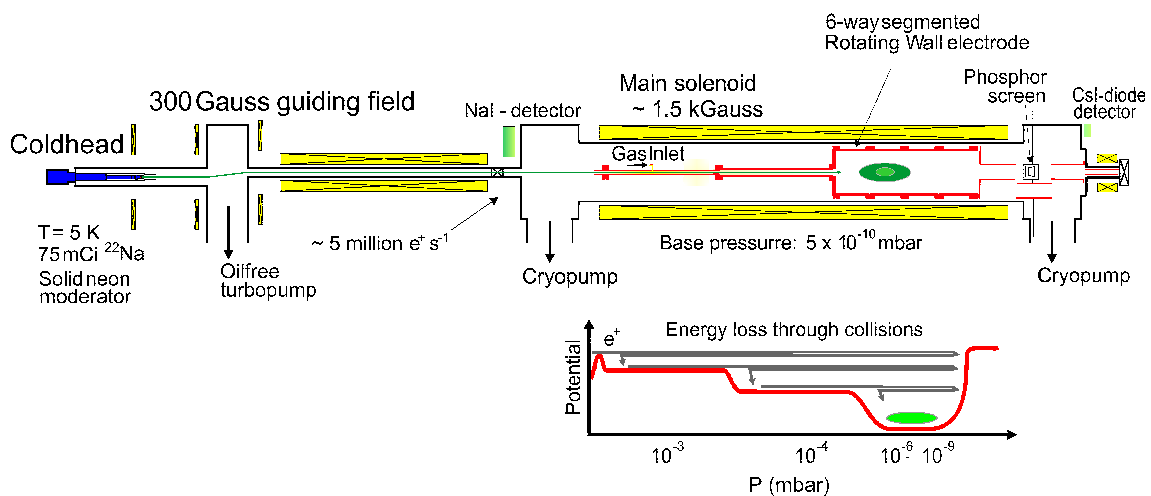


Figure 6. Schematic of the ALPHA positron accumulator. The three stages of the trap (see the lower figure) have progressively lower gas pressures due to differential pumping. The third stage electrodes are around 30 cm in diameter.

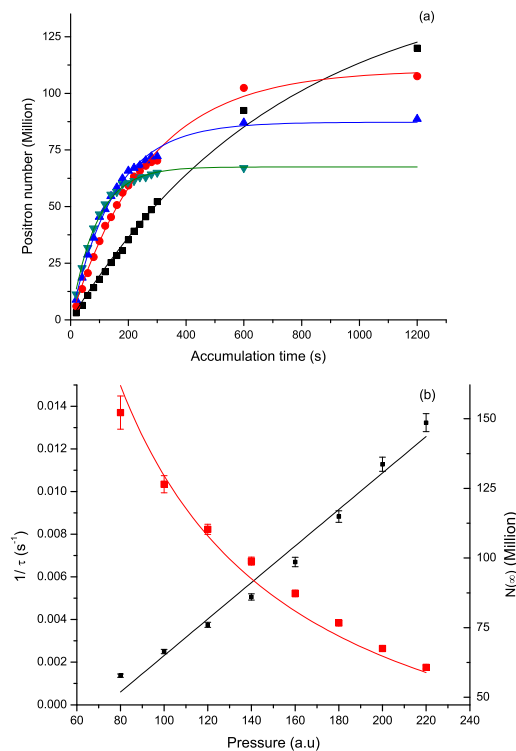


Figure 7. a) Examples of accumulation curves for pressures as measured in the gas supply line of 80 (■), 120 (▼), 160 (▲) and 200 (●) mbar. Note that 100 corresponds to a first stage pressure of around 10^{-3} mbar. b) The variation of $1/\tau$ (black) and $N(\infty)$ (red) with gas pressure, P , together with fits to the expected forms (see text).

plasma, and hence the antiproton, rotational speed is lowered. Furthermore, simulations [6] have found that at high positron densities, the antiprotons undergo rapid antihydrogen formation and re-ionization cycles, which effectively transports them across the magnetic field lines to the edge of the plasma. Here, the weakly bound states that result from the three-body antihydrogen formation reaction (see below) are mostly field ionized by the plasma electric fields, such that the antihydrogen yield is depressed. Higher positron densities also mean higher space charge potentials. The desire to control antiproton-positron interactions on the degree-K level, in the presence of space charge measured in terms of eV, is a challenge. Thus, ALPHA has devised a method of cutting the positron ensemble into two, and discarding one of the halves. In principle, this can be carried out many times, though a reduction by a factor of 4 is typical. The sequence of positron manipulations, from the accumulator to preparation for mixing, takes around 400 s in total.

Returning to the positron accumulator, the performance of this instrument has been investigated from time-to-time over the years. The accumulation rate, R , from the low energy beam is a constant and given by $R = \epsilon I_0$, where I_0 is the intensity of the moderated beam. Thus, the time dependence of the number of accumulated positrons will be $N(t) = N(\infty)(1 - e^{-t/\tau})$, where the saturation limit $N(\infty) = R\tau$. It has been argued elsewhere [44] that this can be written as $N(\infty) = f_{ex} I_0 (1 - e^{-DP}) / BP$, where f_{ex} is the branching ratio for positron capture into the trap (essentially a ratio of scattering cross sections), P is the nitrogen gas pressure and D and B are constants. The factor $(1 - e^{-DP})$ accounts for the attenuation of the positron beam and $1/\tau = BP$: note that strictly the “ P ” in the exponential factor relates to that in the first

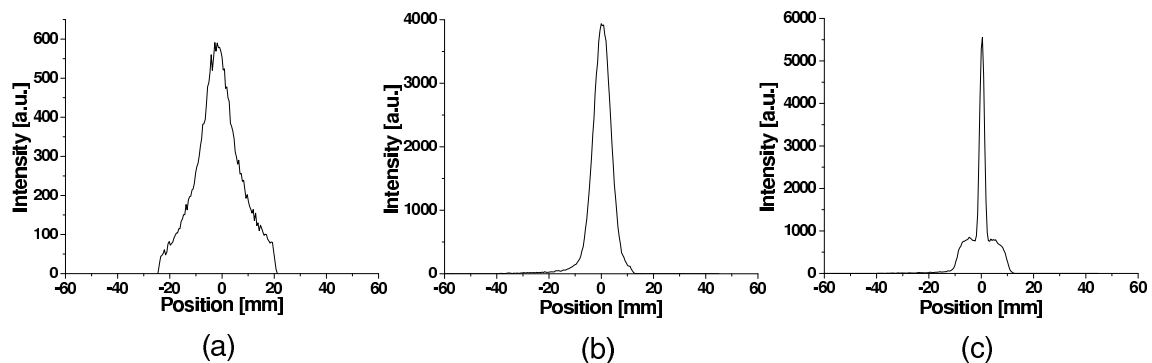


Figure 8. One dimensional projection of the phosphor screen image of the ejected positron cloud following dipolar rotating wall compression. (Note that the overall distribution is ellipsoidal.) (a) no rotating wall; (b) rotating wall with N_2 gas only and (c) rotating wall with N_2 and added CO_2 cooling gas. The integrated yields are around 29, 38 and 30 million positrons for (a), (b) and (c) respectively.

stage of the trap, where the primary scattering event takes place, whilst the “ P ” in BP refers to the third stage, where the particles are stored. When only nitrogen gas is used, the pressures are related, since the gas is admitted into the first stage and the pressure in the third stage is proportional, since molecular flow conditions prevail.

The expression for $N(\infty)$ tends to a constant value of $f_{ex}I_0D/B$ for $DP \ll 1$, whilst for $DP \gg 1$, $N(\infty) \rightarrow f_{ex}I_0/BP$. The quantity B is related to the particle loss via annihilation and possibly radial transport in the trap (the latter can be arrested by the application of a rotating wall) and can be derived from experiments measuring $N(t)$ versus P . The beam intensity, I_0 , can be determined using a calibrated detector, leading to a value for f_{ex} . This was found earlier [44] to be ~ 0.4 . Examples of curves of $N(t)$ versus t and $N(\infty)$ and $1/\tau$ versus P are given in figure 7, showing that the ALPHA 3-stage accumulator behaves according to expectations, at least over the main pressure range of its application. (Note the offset pressure range in Figure 7. Data at lower pressure seem to indicate that the accumulator has another mode of operation, which will be investigated in future.)

Figure 8 shows the spatial profile of the positron cloud ejected from the accumulator both without the rotating wall compression and for two cases with the rotating wall applied. Here a segmented electrode located in the third stage of the accumulator configured in a dipolar mode was used to apply the rotating wall. It is clear from the figure that the rotating wall substantially increases the central density of the plasma. This is desirable, as smaller radius positron plasmas can be created on transfer to the main mixing magnet for antihydrogen production.

4. Antihydrogen production in a magnetic minimum trap

When positrons are mixed with antiprotons under the conditions of the ALPHA experiment, it has long been supposed that two reactions may lead to antihydrogen formation: namely the spontaneous radiative and three-body (two positrons and an antiproton) reactions. It has also been assumed that the three-body reaction would dominate antihydrogen formation, however, as mentioned in the previous section, it has been realised relatively recently [6, 17] that it also results in the transport of the antiprotons to the outskirts of the positron plasma. Depending upon the density of the positrons, this may occur on a timescale as to preclude significant antihydrogen formation via spontaneous radiative recombination. Thus, most of the antihydrogen formed will

be via the reaction



which will produce states bound by around $k_B T_e$, where T_e is the temperature characteristic of the positron plasma. Such weakly bound states are susceptible to field ionization, either from the electric fields associated with the plasma, or the trap fields.

Experience from ATHENA has shown that injection of antiprotons into the positron plasma with kinetic energies in the 10-20 eV range results in spatial annihilation distributions which can only be explained if antihydrogen is formed efficiently by antiprotons which have not thermalised with the positrons [45]. The implications for holding antihydrogen in traps which (for the ground state) are ~ 1 K deep are obvious. There are also several mysteries from the ATHENA data, which are as yet unresolved. Despite the supposed dominance of the three-body reaction (which has a textbook dependence of $T_e^{-9/2}$), attempts to measure the temperature dependence of the antihydrogen formation rate have produced much shallower dependencies, typically $\sim T_e^{-1}$ [46, 47]. Currently this is not understood, and further work is ongoing. Taken together, what we do, and don't, know about the details of antihydrogen formation in strong field Penning-type trap arrangements means that we should have detailed control over the parameters of both the positron and antiproton clouds, including the manner in which they are mixed. The manipulations performed on the positrons and antiprotons have been summarized above.

A distinctive feature of the ALPHA antihydrogen apparatus is, as shown in figure 1, the superposition of a magnetic minimum neutral atom trap onto the charged particle traps used to hold and mix the antiprotons and positrons. As has been elaborated elsewhere [48], ALPHA has created its neutral trap using a pair of mirror coils and an octupolar arrangement to provide the radial confinement. The choice of the latter, over the more familiar quadrupole [15], was motivated by the shallower magnetic field gradient near the axis of the system in the octupolar case, which should result in plasmas with extended lifetimes and greater stability [49, 50]. The magnitude of the depth of the neutral atom trap is given by $U = \mu \Delta B$, where μ is the magnetic moment of the atom, and ΔB is the difference in magnetic field between the point of antihydrogen formation (taken to be approximately on the axis of the system) and the Penning trap electrode wall, located at a radius of around 22 mm. For the ground state of antihydrogen $\mu = \mu_B$, the Bohr magneton, such that the trap depth is ~ 0.7 KT⁻¹. Using state-of-the-art superconducting technology [48], ALPHA has developed a system with around 1 T of field change across the radial extent of its trap, such that ground state atoms with kinetic energies below ~ 0.7 K should be confined.

ALPHA has recently demonstrated the efficient formation of antihydrogen in its combined charged particle/neutral atom trap [17]. It has detected the antihydrogen via its annihilation on the electrode wall, as well as using the field ionization technique developed by ATRAP [2]. Good correlation between these complementary signals has been found [17]. The distributions of the radial and axial annihilation positions of the antihydrogen, as reconstructed using ALPHA's vertex detector [51], are shown in figure 9 for the cases with the neutral trap off, and fully energized. In the former case the annihilation distributions are smooth, though there is some structure in the data with the trap on. It has been argued [17] that this is due to the transport to the wall of antiprotons which have resulted from field ionization of antihydrogen at large radii in the trap. Beyond a critical radius [52], which depends upon the strength of the octupolar field, any field ionized antiprotons will be automatically swept to the wall due to the radial behaviour of the octupolar field. Such a process, as described above, also has support from recent simulations [6], though in the context of the ATHENA experiment.

ALPHA has developed a strategy to search for trapped antihydrogen atoms [53], which it is continuing to refine as the positron and antiproton manipulation techniques described in sections 2 and 3 are fully integrated into the experimental protocol. Briefly, positron-antiproton mixing is performed for about 1 s, whereupon the charged particle traps are emptied. This is followed

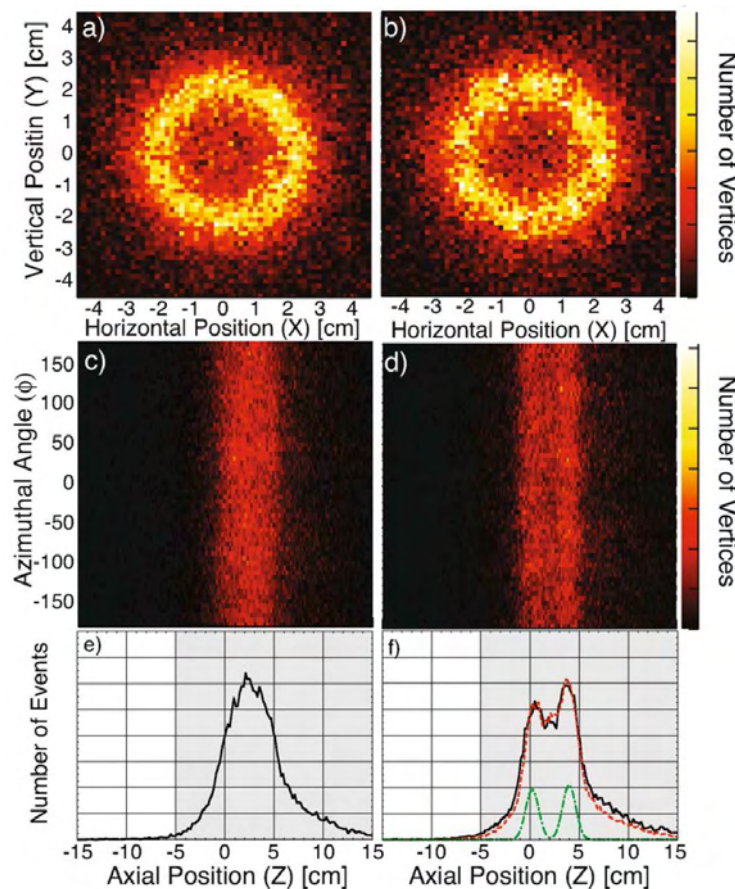


Figure 9. a),b) Azimuthal projections of antihydrogen annihilations with (b) and without (a) the neutral trap energised. (c),(d) and (e),(f) are the corresponding z - ϕ and z -distributions respectively. In (f), the red curve is a fit using a scaled version of (e) together with the two green peaks. The latter are caused by field ionized antihydrogen (see text). When these data were taken the vertex detector was incomplete and had only one layer of silicon modules for the unshaded region. This caused a lower vertex reconstruction efficiency, resulting in the slight asymmetry of the distributions evident in (e) and (f).

by a deliberate quench of the neutral atom trap. The current from the coils is dumped into a resistive load and the $1/e$ time for the decay is just under 10 ms [53]. ALPHA then searches the output of the vertex detector in a time window of 30 ms to look for annihilations which could be characteristic of antihydrogen released from the neutral atom trap. The narrow time window is an effective veto for cosmic ray events [54]. Work is ongoing.

5. Concluding remarks

We have described how antiprotons and positrons can be manipulated using a number of advanced techniques, before being combined to form antihydrogen. Current efforts to trap antihydrogen atoms have been discussed in the context of the ALPHA experiment, which is located at the unique AD facility at CERN. The motivation for attempting these difficult experiments was briefly sketched.

6. Acknowledgements

Our work has been supported by a number of national funding agencies. We are grateful to: EPSRC and the Leverhulme Trust (UK); CNPq and FINEP (Brazil); ISF (Israel); FNU (Denmark); VR (Sweden); NSERC, NRC/TRIUMF and AIF (Canada); DOE and NSF (USA). We are very appreciative of the support we receive at CERN.

7. References

- [1] Amoretti M *et al* (ATHENA collaboration) 2002 *Nature* **419** 456
- [2] Gabrielse G *et al* (ATRAP collaboration) 2002 *Phys. Rev. Lett.* **89** 213401
- [3] Holzschleiter M H, Charlton M and Nieto M M 2004 *Phys. Rep.* **402** 1
- [4] Gabrielse G 2005 *Adv. At. Mol. Opt. Phys.* **50** 155
- [5] Robicheaux F 2008 *J. Phys. B: At. Mol. Opt. Phys.* **41** 192001
- [6] Jonsell S, van der Werf D P, Charlton M and Robicheaux F 2009 *J. Phys. B: At. Mol. Opt. Phys.* **42** 215002
- [7] Niering M *et al* 2000 *Phys. Rev. Lett.* **84** 5496
- [8] Essen L, Donaldson P W, Bangham M J and Hope E G 1971 *Nature* **229** 110
- [9] Kellerbauer A *et al* (AEGIS collaboration) 2008 *Nuc. Inst. Meth. in Phys. Res. B* **226** 351
- [10] Pérez P *et al* in *Cold Antimatter Plasmas and Application to Fundamental Physics* (AIP Conf. Proc. **1037**) Eds Y. Kanai and Y. Yamazaki (2008) p. 35
- [11] Bluhm R, Kostelecký V A and Russell N 1997 *Phys. Rev. Lett.* **79** 1432
- [12] Bluhm R, Kostelecký V A and Russell N 1999 *Phys. Rev. Lett.* **82** 2254
- [13] Bluhm R 2004 *Nuc. Inst. Meth. in Phys. Res. B* **221** 6
- [14] Shore G M 2005 *Nuc. Phys. B* **717** 86
- [15] Pritchard D E 1983 *Phys. Rev. Lett.* **51** 1336
- [16] Gabrielse G *et al* (ATRAP collaboration) 2008 *Phys. Rev. Lett.* **100** 113001
- [17] Andresen G B *et al* (ALPHA collaboration) 2010 *Phys. Lett. B* **685** 141
- [18] Maury S 1997 *Hyperfine Interact.* **109** 43
- [19] Gabrielse G *et al* 1986 *Phys. Rev. Lett.* **57** 2504
- [20] Beck B R, Fajans J and Malmberg J H 1996 *Phys. Plasmas* **3** 1250
- [21] Malmberg J H and Driscoll C F 1980 *Phys. Rev. Lett.* **44** 654
- [22] Notte J and Fajans 1994 *Phys. Plasmas* **1** 1123
- [23] Gabrielse *et al* (TRAP collaboration) 1989 *Phys. Rev. Lett.* **63** 1360
- [24] see eg Andresen G B *et al* 2008 *J. Phys. B: At. Mol. Opt. Phys.* **41** 011001
- [25] Huang X P, Anderegg F, Hollman E M, Driscoll C F and O'Neil T M 1997 *Phys. Rev. Lett.* **78** 875
- [26] Anderegg F, Hollman E M and Driscoll C F 1998 *Phys. Rev. Lett.* **81** 4875
- [27] Greaves R G and Surko C M 2000 *Phys. Rev. Lett.* **85** 1883
- [28] Danielson J R and Surko C M 2005 *Phys. Rev. Lett.* **94** 035001
- [29] Danielson J R, Surko C M, and O'Neil T M 2007 *Phys. Rev. Lett.* **99** 135005
- [30] Jørgensen L V *et al* (ATHENA collaboration) 2005 *Phys. Rev. Lett.* **95** 025002
- [31] Funakoshi R *et al* (ATHENA collaboration) 2007 *Phys. Rev. A* **76** 012713
- [32] Andresen G B *et al* 2008 *Phys. Rev. Lett.* **100** 203401
- [33] Andresen G B *et al* 2010 *Phys. Rev. Lett.* **105** 013003
- [34] Eggleston D L, Driscoll C F, Beck B R, Wyatt A and Malmberg J H 1992 *Phys. Fluids* **4** 3432
- [35] Amoretti M *et al* (ATHENA collaboration) 2004 *Nuc. Inst. Meth. in Phys. Res. A* **518** 679
- [36] Khatri R, Charlton M, Sferlazzo P, Lynn K G, Mills Jr A P and Roellig L O 1990 *Appl. Phys. Lett.* **57** 2374
- [37] Mills Jr A P, and Gullikson E M 1986 *Appl. Phys.* **49** 1121
- [38] Surko C M, Passner A, Leventhal M and Wysoki F J 1988 *Phys. Rev. Lett.* **61** 1831
- [39] Murphy T J and Surko C M 1992 *Phys. Rev. A* **46** 5696
- [40] Surko C M and Greaves R G 2004 *Phys. Plasmas* **11** 2333
- [41] Greaves R G and Surko C M 2001 *Phys. Plasmas* **8** 1879
- [42] Al Qaradawi I, Charlton M, Borozan I and Whitehead R 2000 *J. Phys. B: At. Mol. Opt. Phys.* **33** 2725
- [43] Surko C M, Greaves R G and Charlton M 1997 *Hyperfine Interact.* **109** 181
- [44] Clarke J C, van der Werf D P, Griffiths B, Beddows D C S, Charlton M, Telle H H and Watkeys P R 2006 *Rev. Sci. Inst.* **77** 063302
- [45] Madsen N *et al* (ATHENA collaboration) 2005 *Phys. Rev. Lett.* **94** 033403
- [46] Amoretti M *et al* (ATHENA collaboration) 2004 *Phys. Letts B* **583** 59
- [47] Fujiwara M C *et al* (ATHENA collaboration) 2008 *Phys. Rev. Lett.* **101** 053401
- [48] Bertsche W *et al* (ALPHA collaboration) 2006 *Nuc. Inst. Meth. in Phys. Res. A* **566** 746
- [49] Fajans J, Bertsche W, Burke K, Chapman S F and van der Werf D P 2005 *Phys. Rev. Lett.* **95** 155001

- [50] Andresen G B *et al* (ALPHA collaboration) 2007 *Phys. Rev. Lett.* **98** 023402
- [51] Fujiwara M C *et al* in *Cold Antimatter Plasmas and Application to Fundamental Physics* (AIP Conf. Proc. **1037**) Eds Y. Kanai and Y. Yamazaki (2008) p. 208
- [52] Fajans J, Madsen N and Robicheaux F 2008 *Phys. Plasmas* **15** 032108
- [53] Andresen G B *et al* in *Cold Antimatter Plasmas and Application to Fundamental Physics* (AIP Conf. Proc. **1037**) Eds Y. Kanai and Y. Yamazaki (2008) p. 241
- [54] Butler E *et al* 2010 to appear in *Hyperfine Interactions*